Nonlinear X-shaped waves by second-harmonic generation with collimated femtosecond pulses

Wenqi Lei,[1] Jian Wu,[1,2] Hua Cai,[1] and Heping Zeng[1,3]

[1]*State Key Laboratory of Precision Spectroscopy, East China Normal University, Shanghai 200062, China*
[2]*jwu@phy.ecnu.edu.cn*
[3]*hpzeng@phy.ecnu.edu.cn*

Received August 11, 2008; revised November 22, 2008; accepted November 28, 2008;
posted December 9, 2008 (Doc. ID 100017); published January 13, 2009

Nonlinear X-shaped angle-wavelength spectrum of the generated second-harmonic wave is observed for a collimated femtosecond pulse of a large beam waist, where the spatiotemporal balance is originated from mutual coupling of the effective nonlinear Kerr effects, pulse frequency chirp, and negative phase shift from cascaded quadratic processes with appropriate phase mismatch. © 2009 Optical Society of America

OCIS codes: 320.7120, 190.3270, 320.2250, 190.2620.

The study of cascaded second-order nonlinear processes in quadratic media [1] has attracted much attention, since it can be equivalent to an effective third-order process with a quite high nonlinearity and can be controlled by varying the phase mismatch between the involved waves. The strong optical nonlinearities can also be used to suppress the spatial diffraction or the temporal dispersion of an intense optical pulse, leading to the formation of optical solitons [2]. For ultrashort pulses, the strong spatiotemporal couplings have been extensively studied as spatiotemporal modulation instability [3,4], nonlinear X-shaped waves [5], self-mode-locking of ultrafast solid-state lasers [6], and so forth. Nonlinear X-shaped waves have been observed with filamentation [7] and second-harmonic generation (SHG) processes [8] owing to the strong interplay of the diffraction, dispersion, and the nonlinear Kerr effect [9,10], where tightly focused ultrashort laser pulses with quite small beam waists were used as the inputs to ensure dispersion and diffraction lengths comparable to the effective nonlinear length.

In this Letter, we demonstrate that a nonlinear X-shaped wave can be generated by SHG with a collimated femtosecond pulse of a large beam waist, rather than a tightly focused one. Instead of the material dispersion and diffraction, the accumulated nonlinear phase shift from the cascaded second-order processes with an amount of phase mismatch and the intrinsic frequency chirp of incident pulse play dominate roles in counteracting the optical nonlinearities to form an X-shaped wave.

An output from an amplified Ti:sapphire laser system (repetition rate ~1 kHz, pulse width ~40 fs, beam radius ~2.5 mm, central wavelength ~800 nm) was collimated (reduction factor of 10:3) and steered into a 4-mm-long β-barium borate (BBO) crystal for type-I SHG of the fundamental wave (FW), which was positively chirped with effective pulse durations from 40 to 770 fs. The phase mismatch between the FW and the second harmonic (SH) was controlled by adjusting the angle between the incident FW and the axis of the BBO crystal. By using a Fourier lens, the output beam was first transformed to the surface of a slit to obtain the spatial angular distribution (θ), which was then diffracted by a grating after another lens to produce the wavelength distribution (λ). Finally, the reconstructed angle-wavelength (θ–λ) spectrum was recorded by a commercial CCD with an exposure time of 0.9 ms to ensure a single-shot measurement. Here, only the SH wave was recorded with a short-pass filter (Thorlabs FES0550) before the CCD; please note that all the figures throughout this Letter are presented in a linear scale.

Figure 1 shows the measured (θ–λ) spectra of the SH wave driven by FW pulses with chirps as $C \sim 0$, 9.8×10^{-6}, 1.9×10^{-5}, 3.2×10^{-5} fs^{-2} from Figs. 1(a)–1(d), where C is related to the pulse duration τ_p and chirp-free pulse duration τ_0 through $\tau_0=\tau_p/(1+C^2\tau_{pm}{}^4)^{1/2}$, with $\tau_{pm}=770$ fs [11,12]. The phase

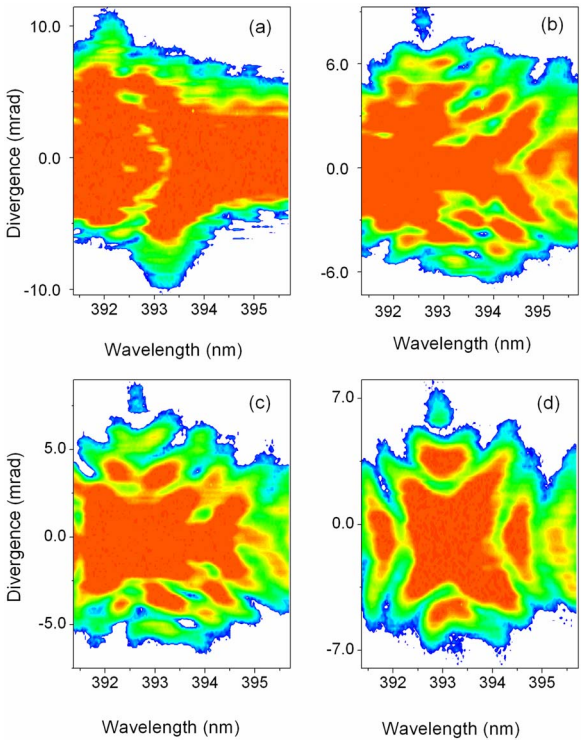

Fig. 1. (Color online) Measured (θ–λ) spectra of the SH waves under various durations of the incident FW pulse as (a) $\tau_p=41$, (b) $\tau_p=234$, (c) $\tau_p=455$, and (d) $\tau_p=770$ fs, respectively.

mismatch was adjusted to be $\Delta k = k_{2\omega} - 2k_{\omega} \sim 1.3 \times 10^3$ cm^{-1}, where k_{ω} and $k_{2\omega}$ are the wave vectors of the FW and SH waves, respectively. The X-shaped wave emerged only as an adequate positive chirp was preintroduced to the incident pulse, and, as shown in Fig. 1(d), a clear X-shaped (θ–λ) spectrum was observed with a positive chirp of $C \sim 3.2 \times 10^{-5}$ fs^{-2}. With an incident beam radius of $w_0 = 0.75$ mm and a pulse duration of $\tau_p = 770$ fs, the corresponding diffraction and dispersion lengths were estimated to be $L_{\mathrm{df}} = k_{\omega} w_0^2/2 \sim 367$ cm and $L_{\mathrm{ds}} = 0.322\tau_p^2/(d^2k_{\omega}/d\omega^2)|_{\omega} \sim 255$ cm, which were much larger than the length of the BBO crystal used in our experiments. Meanwhile, the nonlinear length was estimated to be $L_{\mathrm{nl}} = n_{\omega}\lambda/\pi\chi^{(2)}E_0 \sim 0.01$ cm, where n_{ω}, λ, and E_0 are, respectively, the linear refractive index, central wavelength, and amplitude of the FW pulse, and $\chi^{(2)}$ is the second-order nonlinear optical susceptibility. Hence, the effects of the diffraction and the dispersion could be neglected and could not counteract the nonlinear Kerr effect at all. Here, in the normal dispersion region, the temporal dispersion of the ultrashort pulse was increased with a preintroduced positive chirp, which thus equivalently shortened the dispersion length [13] and then balanced the Kerr nonlinearities. We also tried the measurements with negatively prechirped incident pulses. No evident X-shaped wave was observed, since the corresponding dispersion length was increased for a negatively chirped pulse in a normally dispersive medium. The preintroduced positive pulse chirp not only shortened the dispersion length but also decreased the pulse intensity and the corresponding nonlinear Kerr effects.

Actually, the negative phase shift from the cascaded quadratic processes has the same effect as the spatial diffraction and can be used to compensate for the self-focusing of the beam. Figure 2 shows the measured (θ–λ) spectra of the SH wave as the increasing phase mismatches from 984.1 to 1.9×10^3 cm^{-1} for a fixed pulse chirp of $C = 3.2 \times 10^{-5}$ fs^{-2}. The X-shaped tails emerged only with sufficient phase mismatches, i.e., $\Delta k \geqslant 984.1$ cm^{-1}. The self-focusing and self-phase modulation in media with a nonlinear refractive index $n_2 > 0$ arise from the nonlinear phase shift $\Phi_{\mathrm{kerr}}(x,y) = (2\pi/\lambda) \times \int n_2(z) I(x,y,z) \mathrm{d}z$, referred as the B integral [14]. The phase shift accumulated from cascaded nonlinear processes in quadratic media reads $\Phi_{\mathrm{nl}} \approx -(\Gamma^2 L^2)/(\Delta k \times L)$ [14] with the crystal length L and $\Gamma = (\omega\chi^{(2)}|E_0|)/[2_{C_0}(n_{\omega}n_{2\omega})^{1/2}]$. With a phase mismatch of $\Delta k \sim 1.3 \times 10^3$ cm^{-1}, the nonlinear phase shift from the cascaded quadratic processes is estimated to be $\Phi_{\mathrm{nl}} \sim -0.89\pi$, which is comparable to the phase shift induced by the B integral $\Phi_{\mathrm{kerr}} \sim 0.62\pi$. The negative phase shift from the cascaded quadratic processes decreases the effective diffraction length and compensates for the self-focusing effect, leading to the observation of X-shaped waves in our experiments. Under the optimal pulse chirp of $C = 3.2 \times 10^{-5}$ fs^{-2} and phase mismatch of $\Delta k \sim 1.3 \times 10^3$ cm^{-1}, the dependence of the X-shaped waves on the driving intensity was studied by slowly increasing the incident power

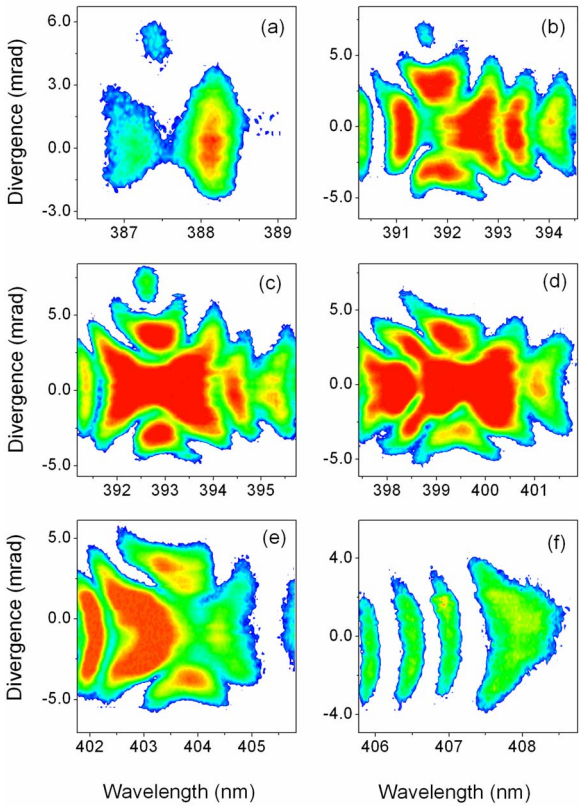

Fig. 2. (Color online) Measured (θ–λ) spectra of the SH waves under different phase mismatches Δk with corresponding nonlinear phase shifts Φ_{nl} in brackets as (a) 9.841×10^2 cm^{-1} (-1.186π), (b) 1.212×10^3 cm^{-1} (-0.963π), (c) 1.311×10^3 cm^{-1} (-0.890π), (d) 1.541×10^3 cm^{-1} (-0.757π), (e) 1.740×10^3 cm^{-1} (-0.670π), and (f) 1.941×10^3 cm^{-1} (-0.601π).

of the FW as shown in Fig. 3. The X-shaped (θ–λ) spectrum could be observed only as the driving FW intensity was larger than 37.0 GW/cm^2, where sufficient spectral broadening of the SH wave and cascaded quadratic nonlinear processes could result to compensate for the phase shift induced by the B integral. Similar to the generation of an X-shaped wave by using a tightly focused beam, spectral broadening is important for the observed X-shaped wave here. In fact, in our experiments, the input wavelength of the FW covered from 780 to 815 nm and the output SH spectrum covered from 380 to 410 nm, which was actually broadened during the complicated cascaded quadratic nonlinear processes. However, the CCD used in the experiment was not large enough to catch the whole spectrum, and only the center part of the spectrum was chosen. The periodicities in the spectral partitions indicate a temporal split of the generated SH wave as a result of the cascaded processes in the presence of phase and group-velocity mismatches [15], which becomes clearer as the increasing phase mismatch as shown in Fig. 2.

The physical underlying of the observed X-shaped wave with a collimated femtosecond pulse is confirmed by numerically integrating the coupled-wave equations [16] by including the cross-phase modulation between the FW and the SH waves. As shown in Fig. 4, the X-shaped wave can be observed only for

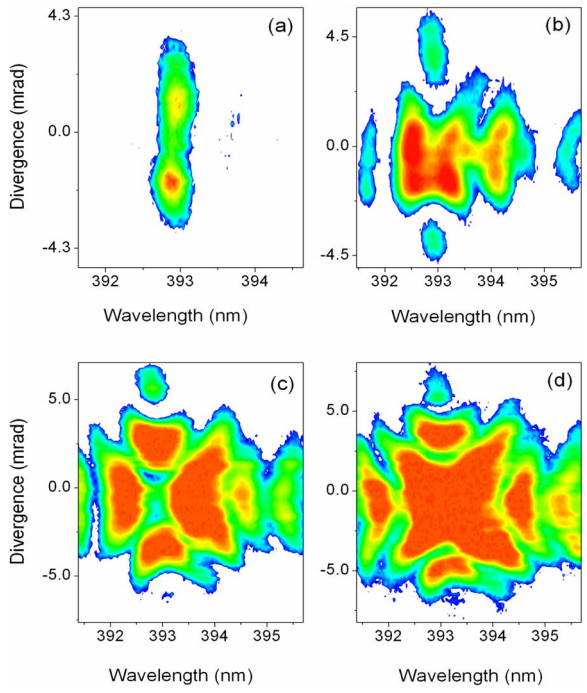

Fig. 3. (Color online) Measured (θ–λ) spectra of the SH waves under different FW intensities as (a) 11.6, (b) 37.0, (c) 86.7, and (d) 124.9 GW/cm^2.

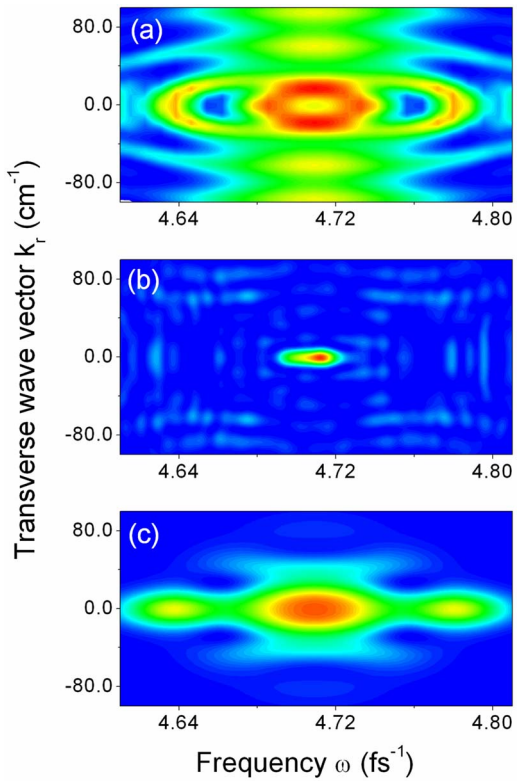

Fig. 4. (Color online) Simulated (θ–λ) spectra of the SH waves under various durations of the incident FW pulse and phase mismatches as (a) $\tau_p = 40$ fs, $\Delta k = 1.0 \times 10^3$ cm^{-1}, (b) $\tau_p = 600$ fs, $\Delta k = 0$ cm^{-1}, and (c) $\tau_p = 600$ fs, $\Delta k = 1.0 \times 10^3$ cm^{-1}.

sufficiently positive chirp and evident phase mismatch in the frequency-doubling process. This agrees well with our experimental observation that an amount of positive chirp together with well-compensated nonlinear phase shifts from phase mismatch are necessary to suppress the strong nonlinearity and lead to the formation of an X-shaped wave.

In summary, nonlinear X-shaped waves were observed in a quadratic nonlinear medium under the circumstance of imbalanced interplay of dispersion, diffraction, and optical nonlinearities. In a phase-mismatched SHG driven by a collimated femtosecond pulse of a large beam waist, the temporal dispersion was increased by preintroducing an appropriate positive chirp, and the spatial diffraction was modified by the phase shift accumulated from the cascaded quadratic nonlinear processes, leading to counterbalance between optical nonlinearities and dispersion (diffraction) to form an X-shaped wave. This is quite different from the conventional one induced by a tightly focused beam and presents a significant way to understand the nonlinear X-shaped waves.

This work was funded in part by National Natural Science Fund (grants 10525416 and 10804032), National Key Project for Basic Research (grant 2006CB806005), Projects from Shanghai Science and Technology Commission (grants 06JC14025 and 08ZR1407100), Program for Changjiang Scholars and Innovative Research Team in University, and Shanghai Educational Development Foundation (grant 2008CG29).

References

1. Y. Wang, J. Campos, C. Xu, S. Yang, E. Ponomarev, and X. Bao, Appl. Opt. **45**, 5391 (2006).
2. G. Assanto and G. Stegeman, Opt. Express **10**, 388 (2002).
3. S. Akturk, X. Gu, P. Gabolde, and R. Trebino, Opt. Express **13**, 8642 (2005).
4. H. Zeng, J. Wu, H. Xu, K. Wu, and E. Wu, Phys. Rev. Lett. **92**, 143903 (2004).
5. C. Conti and S. Trillo, Opt. Lett. **28**, 1251 (2003).
6. H. Wu, C. Huang, and J. Huang, Opt. Express **15**, 2391 (2007).
7. B. Prade, M. Franco, A. Mysyrowicz, A. Couairon, H. Buersing, B. Eberle, M. Krenz, D. Seiffer, and O. Vasseur, Opt. Lett. **31**, 2601 (2006).
8. P. Larsen, M. Sørensen, O. Bang, W. Królikowski, and S. Trillo, Phys. Rev. E **73**, 036614 (2006).
9. C. Conti, Phys. Rev. E **68**, 016606 (2003).
10. M. Kolesik, E. Wright, and J. Moloney, Phys. Rev. Lett. **92**, 253901 (2004).
11. R. Nuter, S. Skupin, and L. Bergé, Opt. Lett. **30**, 917 (2005).
12. L. Torner, C. Menyuk, and G. Stegeman, Opt. Lett. **19**, 1615 (1994).
13. A. Ryan and G. Agrawal, J. Opt. Soc. Am. B **12**, 2382 (1995).
14. K. Beckwitt, F. Wise, L. Qian, L. Walker II, and E. Canto-Said, Opt. Lett. **26**, 1696 (2001).
15. W. Su, L. Qian, H. Luo, X. Fu, H. Zhu, T. Wang, K. Beckwitt, Y. Chen, and F. Wise, J. Opt. Soc. Am. B **23**, 51 (2006).
16. X. Liu, K. Beckwitt, and F. Wise, Phys. Rev. E **62**, 1328 (2000).